Chapter 17
Wave Filtering and Dynamic Positioning of Marine Vessels Using a Linear Design Model: Theory and Experiments

V. Hassani and A.M. Pascoal

Abstract This chapter describes a procedure to obtain an improved design model of ships subjected to the influence of currents and sea waves. The model structure is at the heart of the application of new techniques in control and estimation theory to the problem of Dynamic Positioning (DP) and wave filtering of marine vessels. The model proposed captures the physics of the problem at hand in an effective manner and includes the sea state as an uncertain parameter. This allows for the design of advanced control and estimation algorithms to solve the DP and wave filtering problems under different sea conditions. Numerical simulations, carried out using a high fidelity nonlinear DP system simulator, illustrate the performance improvement in wave filtering as a result of the use of the proposed model. Furthermore, using Monte-Carlo simulations the performance of three DP controllers, designed based on the plant model developed, is evaluated for different sea conditions. The first controller is a nonlinear multivariable PID controller with a passive observer. The second controller is of the Linear Quadratic Gaussian type and the third controller builds on $\mathcal{H}_\infty$ control techniques using the mixed-μ synthesis methodology. The theoretical results are experimentally verified and the performance of wave filtering in DP systems operated with the controllers designed for different sea conditions are further examined by model testing a DP operated ship, the Cybership III, in a towing tank equipped with a hydraulic wavemaker.

V. Hassani (✉)
Department of Marine Technology, Norwegian Marine Technology Research Institute (MARINTEK) and Centre for Autonomous Marine Operations and Systems (AMOS), Norwegian University of Science and Technology, Trondheim, Norway
e-mail: Vahid.Hassani@ntnu.no

A.M. Pascoal
Laboratory of Robotics and Systems in Engineering and Science, Instituto Superior Técnico, University of Lisbon, Lisbon, Portugal
e-mail: Antonio@isr.ist.utl.pt

17.1 Introduction

The first step in the design of a control system or observer for a marine vessel, transporting and operating over water, is the development of a model describing the dynamic behavior of the ship and its interaction with the environment that captures the influence of waves and currents. An appropriate control design model should be simple enough and yet reflect the main physical characteristics of the plant at hand. A controller designed using a model of this type will inherit structural information about the physical properties of the plant and has the potential to achieve good performance and robustness properties, if at all possible. This chapter is devoted to derive such a control design model that satisfies the above properties and can therefore be used for efficient design of Dynamic Positioning (DP) systems. The latter started to appear in the 1960s for offshore drilling applications, due to the need to drill in deep waters and the realization that Jack-up barges and anchoring systems could not be used economically at such depths. Nowadays, many types of marine vessels such as drilling, pipe laying, crane, supply, passenger, and cruise vessels are equipped with a DP systems [27]. Early DP systems were implemented using PID controllers. In order to restrain thruster trembling caused by the wave-induced motion components, notch filters in cascade with low pass filters were used with the controllers [6]. However, notch filters restrict the performance of closed-loop systems because they introduce phase lag about the crossover frequency, which in turn tends to decrease phase margin. An improvement in the performance obtained with DP controllers was achieved by exploiting more advanced control techniques based on optimal control and Kalman filter theory, see [1]. These techniques were later modified and extended in [2, 3, 5, 10–13, 25, 28, 30, 32]. For a survey of DP control systems, see for example [27] and the references therein.

One of the most fruitful concepts introduced in the course of the body of work referred above is that of wave filtering, together with the strategy of modeling the total vessel motion as the superposition of low-frequency (LF) and wave-frequency (WF) vessel motions. It was further recognized that in order to reduce the mechanical wear and tear of the propulsion system components, in small to high sea states, the estimates entering the DP control feedback loop should be filtered by using a so-called wave filtering technique so as to prevent excessive control activity in response to WF components. In practice, position and heading measurements are corrupted with sensor noise. Furthermore, measured position and heading reflect the impact of external disturbances such as waves and ocean currents acting on the vessel. The need therefore arises for an observer to achieve wave filtering and "separate" the LF and WF position and heading estimates (see [6] for details). In extreme seas or swell with very long wave periods, wave filtering is turned off as described in [17, 21, 27].

In [28], WF filtering was done by exploiting the use of Kalman filter theory under the assumption that the kinematic equations of the ship's motion can be linearized about a set of predefined constant yaw angles (36 operating points in steps

of 10°, covering the whole heading envelope); this is necessary when applying linear Kalman filter theory and gain scheduling techniques. However, global exponential stability of the complete system cannot be guaranteed. In [9], a nonlinear observer with wave filtering capabilities and bias estimation was designed using passivity methods. An extension of this observer with adaptive wave filtering was described in [31]. Gain-scheduled wave filtering was introduced in [32].

To the best of our knowledge, in the wave filtering techniques described in the above mentioned references the WF components of marine vessel motion are computed in a earth-fixed frame (also denoted as North-East-Down frame), while the hydrodynamic forces and torques acting on the vessel are naturally given (via the corresponding hydrodynamic coefficients) in terms of variables that are best measured in body-axis (because they capture the influence between the vessel and the environment locally, no matter what the attitude of the vessel is, in inertial coordinates). Assuming a stationary wave pattern, this suggests that the WF motions should be modeled in a hydrodynamic frame (or body frame) rather than in a North-East-Down frame. This observation is at the root of the new linear model adopted in this Chapter both for control and wave filtering purposes.

From a practical standpoint, this chapter is strongly motivated by the need to develop high performance Dynamic Positioning (DP) systems. The latter have traditionally been for low-speed applications, where the basic DP functionality is either to keep a fixed position and heading of a ship, or to move it slowly from one location to another. In this work, using a low speed assumption, a linear model of a vessel is developed that captures practical aspects and plays a central role in the design of control and estimation algorithms for DP and wave filtering of marine vessels in presence of sea waves and disturbances. The main emphasis of the chapter is on the new linear model proposed; to show the usefulness of the model, two wave filters are designed, one based on the model proposed and the other on a commonly used model, after which their performance is compared. The new model can also be used for control systems design. This is illustrated with the design and the evaluation of three classes of DP controllers operating under four different sea conditions: calm, moderate, high, and extreme seas. The first class of controllers is a nonlinear multivariable PID (designed based on a nonlinear plant model). In this setup, a nonlinear passive observer is used for wave filtering. The observer provides estimates of the LF components of position and velocity of the vessel that are used in the controller. Four different nonlinear PID controllers are designed, covering the sea conditions from calm to extreme seas. The remaining two types of controllers are designed based on the new linear model presented. The second class of controllers is of the Linear Quadratic Gaussian (LQG) type. It consists of a steady state Kalman filter and a linear quadratic (state-feedback) controller. As in the previous case, four different LQG controllers are designed covering different sea conditions. The third class of controllers builds on $\mathcal{H}_\infty$ control techniques; four $\mathcal{H}_\infty$ robust controllers are designed for different sea conditions.

The performance of the controllers derived is evaluated with the help of Monte Carlo simulations performed under different environmental conditions, from calm to

extreme seas, using the Marine Cybernetics Simulator (MCSim) [29]. Experimental model tests are also carried out using the Cybership III model vessel of the Marine Cybernetics Laboratory (MCLab) [20].

The structure of the chapter is as follows. Section 17.2 is a brief introduction to important issues that arise in the design of DP systems, followed by the presentation of a new linear vessel model that will be used for filter and control systems design purposes. A brief description of three selected DP control laws (where two of them are designed using the newly proposed vessel model) is given in Sect. 17.2.2. Section 17.3 describes the Marine Cybernetics Simulator and contains the results of numerical Monte-Carlo simulations with stochastic signals that illustrate the performance of the DP controllers and associated estimators under calm to extreme sea conditions. In Sect. 17.4, a short description of the model-test vessel, Cybership III, and experimental results obtained with it are presented. Conclusions and suggestions for future research are summarized in Sect. 17.6.

## 17.2 Dynamic Positioning, Wave Filtering and Ship Modeling

In DP systems, the key objective is to maintain the vessel's heading and position within desired limits. Central to their implementation is the availability of good heading and position estimates, provided by properly designed filters. In general, measurements of the vessel velocities are not available and measurements of position and heading are corrupted with different types of noise. Consequently, the estimates of the velocities must be computed from corrupted measurements of position and heading through a state observer. Furthermore, only the slowly-varying disturbances should be counteracted by the propulsion system, whereas the oscillatory motion induced by the waves (1st-order wave induced loads) should not enter the feedback control loop to prevent excessive control activity in response to WF components of motion. To this effect, DP control systems should be designed so as to react to the LF forces imparted to the vessel only. As mentioned before, wave filtering techniques are exploited to separate the position and heading measurements into LF and WF position and heading estimates. Figure 17.1 illustrates this concept graphically. It was this interesting set of ideas that motivated the work reported in the present chapter on the development of a linear design model for marine vessels with a view to DP and wave filtering applications. In what follows, for the sake of clarity, the vessel model described in [9, 26, 32] is described first. The model admits the realization

$$\dot{\xi}_{\omega} = A_{\omega}(\omega_0)\xi_{\omega} + E_{\omega}w_{\omega}, \tag{17.1}$$

$$\eta_{\omega} = C_{\omega}\xi_{\omega}, \tag{17.2}$$

$$\dot{b} = -T^{-1}b + E_b w_b, \tag{17.3}$$

$$\dot{\eta}_L = R(\psi_L)v_L, \tag{17.4}$$
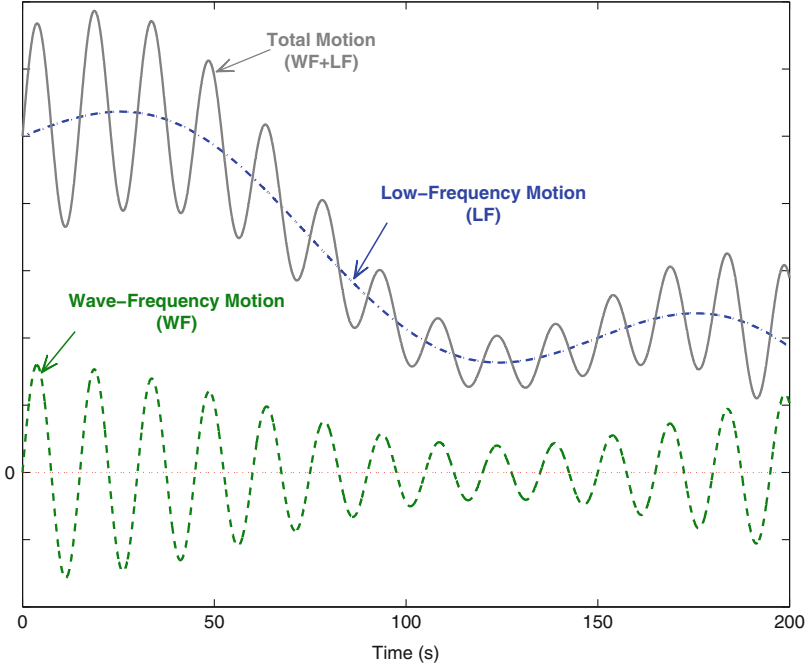
Fig. 17.1 The total motion of a ship is modeled as a LF response with the WF motion added as an output disturbance (adapted from [9, 26])

$$M\dot{v}_L + Dv_L = \tau + R^T(\psi_{tot})b, \tag{17.5}$$

$$\eta_{tot} = \eta_L + \eta_\omega, \tag{17.6}$$

$$\eta_y = \eta_{tot} + v, \tag{17.7}$$

where (17.1) and (17.2) capture the 1st-order wave induced motion in surge, sway, and yaw; (17.3) represents a low order Markov process approximating the slowly varying bias forces (in surge and sway) and torques (in yaw) due to waves (2nd order wave induced loads) and currents, where the latter are given in earth fixed coordinates but later expressed in body-axis in (17.5). Vector $\eta_\omega \in \mathbb{R}^3$ captures the vessel's WF motion due to 1st-order wave-induced disturbances, consisting of WF position (x_W, y_W) and WF heading ψ_W of the vessel; $w_\omega \in \mathbb{R}^3$ and $w_b \in \mathbb{R}^3$ are zero mean Gaussian white noise vectors, and

$$A_\omega = \begin{bmatrix} 0_{3\times3} & I_{3\times3} \\ -\Omega_{3\times3} & -\Lambda_{3\times3} \end{bmatrix}, \qquad E_\omega = \begin{bmatrix} 0_{3\times1} \\ I_{3\times1} \end{bmatrix},$$

$$C_\omega = \begin{bmatrix} 0_{3\times3} & I_{3\times3} \end{bmatrix},$$

with

$$\Omega = \text{diag}\{\omega_{01}^2, \omega_{02}^2, \omega_{03}^2\},$$

$$\Lambda = \text{diag}\{2\zeta_1\omega_{01}, 2\zeta_2\omega_{02}, 2\zeta_3\omega_{03}\},$$

where ω_{0i} and ζ_i are the dominant WF and relative damping ratio, respectively. Matrix $T = \text{diag}(T_x, T_y, T_\psi)$ is a diagonal matrix of positive bias time constants and $E_b \in \mathbb{R}^{3\times3}$ is a diagonal scaling matrix. Vector $\eta_L \in \mathbb{R}^3$ consists of low frequency, earth-fixed position (x_L, y_L) and LF heading ψ_L of the vessel relative to an earth-fixed frame, $\nu_L \in \mathbb{R}^3$ represents the translational and rotational velocities expressed in a vessel-fixed reference frame, and $R(\psi_L)$ denotes a homogeneous transformation given by

$$R(\psi_L) = \begin{bmatrix} \cos(\psi_L) & -\sin(\psi_L) & 0 \\ \sin(\psi_L) & \cos(\psi_L) & 0 \\ 0 & 0 & 1 \end{bmatrix}.$$

Equation (17.5) describes the vessels's LF motion at low speed (see [6]), where $M \in \mathbb{R}^{3\times3}$ is the generalized system inertia matrix including zero frequency added mass components, $D \in \mathbb{R}^{3\times3}$ is a linear damping matrix, and $\tau \in \mathbb{R}^3$ is a control vector of generalized forces generated by the propulsion system, which can produce surge and sway forces as well as a yaw moment. Vector $\eta_{tot} \in \mathbb{R}^3$ represents the vessel's total motion, consisting of total position (x_{tot}, y_{tot}) and total heading ψ_{tot} of the vessel. Finally, (17.7) represents the position and heading measurement equation, where $v \in \mathbb{R}^3$ is zero-mean Gaussian white measurement noise.

Clearly, in the model described in (17.1)–(17.7) the evolution of the WF components of motion, given by (17.1), (17.2) and (17.7), are modeled as a 2nd-order linear time invariant system, driven by Gaussian white noise, in earth-fixed frame.

It is commonly accepted in station keeping operations, assuming small motions about the coordinates η_d (x_d, y_d, and ψ_d), that the coupled equations of WF motions can be formulated in a hydrodynamic frame as[1]

$$M(w)\ddot{\eta}_{R\omega} + D_p(w)\dot{\eta}_{R\omega} = \tau_{\text{wave1}}, \tag{17.8}$$

$$\dot{\eta}_\omega = R(\psi)\dot{\eta}_{R\omega}, \tag{17.9}$$

---

[1]In six degrees-of-freedom dynamics, (17.8) is written as $M(w)\ddot{\eta}_{R\omega} + D_p(w)\dot{\eta}_{R\omega} + G\eta_{R\omega} = \tau_{\text{wave1}}$, where $G \in \mathbb{R}^{6\times6}$ is the linearized restoring coefficient matrix due to the gravity and buoyancy affecting heave, roll, and pitch only (see [26] for more details). Throughout this chapter a three degrees-of-freedom dynamics is used for the design purposes, while a six degrees-of-freedom dynamics is used in the simulation.

where $\eta_{R\omega} \in \mathbb{R}^3$ is the WF motion vector in the hydrodynamic frame, $\eta_\omega \in \mathbb{R}^3$ is the WF motion vector in the Earth-fixed frame, and $\tau_{\text{wave1}} \in \mathbb{R}^3$ is the first order wave excitation vector, which depends on the vessel's heading relative to the incident wave direction. In the above, $M(w) \in \mathbb{R}^{3\times3}$ is the system inertia matrix containing frequency dependent added mass coefficients in addition to the vessel's mass and moment of inertia and $D_p(w) \in \mathbb{R}^{3\times3}$ is the wave radiation (potential) damping matrix. Here, it is assumed that the mooring lines, if any, will not affect the WF motion [33].[2]

The above indicate that the WF motion should be computed in the hydrodynamic frame. We now recall that the problem of modeling the hydrodynamic forces applied to a vessel in regular waves is solved as two sub-problems: "wave reaction" and "wave excitation"; the forces calculated in each of these sub-problems can be added together to give the total hydrodynamic forces [4]. Potential theory is assumed, neglecting viscous effects. The following effects are important:

Wave Reaction, i.e., forces and moments on the vessel when the vessel is forced to oscillate with the wave excitation frequency. The hydrodynamic loads are identified as added mass and wave radiation damping terms.

Wave Excitation, i.e., forces and moments on the vessel when the vessel is restrained from oscillating and there are incident waves. This gives the wave excitation loads which are composed of so-called Froude-Kriloff (forces and moments due to the undisturbed pressure field as if the vessel were not present) and diffraction forces and moments (forces and moments due to the presence of the vessel changes the pressure field).

Results from model tests and computer programs for vessel response analysis often come in the form of transfer functions or tables of coefficients. Similar tools can be applied to study linear wave-induced motions, 2nd-order wave drift, and slowly varying motions. To a large extent, linear theory is sufficient to describe wave-induced motions and loads on vessels. This is especially true for small to moderate sea states.

To this effect, a frequency spectrum $S(\omega)$ is usually selected to describe the energy distribution of the wind generated sea waves and swell over different frequencies, with the integral over all frequencies representing the total energy of the sea state. Common frequency spectra are the Pierson-Moskowitz spectrum, the ISSC spectrum (or modified Pierson-Moskowitz spectrum recommended by International Towing Tank Conference for fully developed sea), the Joint North Sea Wave Project (JONSWAP) spectrum [18], and the more recent doubly peaked spectrum introduced by Torsethaugen (see [6, 26] and the references therein for details). Linear approximations of the wave spectra are studied in the literature; in particular, 2nd-order wave transfer function approximations have been used extensively, see [2, 3, 5, 10–13, 21, 25, 28, 30, 32].

---

[2]It is worth to mention that the evolution of the WF components of motion, given by (17.1) and (17.2), are in fact a simplification of (17.8) and (17.9).

In this work we also consider a 2nd-order wave transfer function approximation and we propose a modified model for the WF components of motion as follows:

$$\dot{\xi}_\omega = A_\omega(\omega_0)\xi_\omega + E_\omega w_\omega, \tag{17.10}$$

$$\eta_\omega = R(\psi_L)C_\omega\xi_\omega, \tag{17.11}$$

$$\dot{b} = -T^{-1}b + E_b w_b, \tag{17.12}$$

$$\dot{\eta}_L = R(\psi_L)v_L, \tag{17.13}$$

$$M\dot{v}_L + Dv_L = \tau + R^T(\psi_{tot})b, \tag{17.14}$$

$$\eta_{tot} = \eta_L + \eta_\omega, \tag{17.15}$$

$$\eta_y = \eta_{tot} + v, \tag{17.16}$$

where all the variables are as defined in (17.1)–(17.7). At this point we would like to highlight the difference between (17.2) and (17.11). As mentioned before, the evolution of the WF components of motion in (17.1), (17.2) and (17.7), are modeled as a 2nd-order linear time invariant system, driven by Gaussian white noise, in earth-fixed frame, while (17.8) suggests that the WF motions be modeled in a body frame. From a physical point of view, it is obvious that the WF motions depend on the angle between the heading of the vessel and the direction of the wave. Assuming stationary waves,[3] one can assume that a linear approximation can be used to described wave-induced motions in the body frame. This justifies the modification applied in (17.11). Modeling the WF motions in earth-fixed frame means that every time a new command for a desired heading is issued, the WF motion dynamic should be updated. By modeling the WF motion dynamics in the body frame this is avoided entirely.

17.2.1 A New Linear Design Model

For low speed DP and wave filtering applications, the following assumptions can be made (these assumptions are widely used in the literature, see [5, 19, 30–32]):

Assumption 1. Position and heading sensor noise are neglected, that is $v = 0$, since the measurement error induced by measurement noise is negligible compared to the wave-induced motion.

Assumption 2. The amplitude of the wave-induced yaw motion ψ_ω is assumed to be small, that is, less than 2–3° during normal operation of the vessel and less than 5°

---

[3]In long-crested irregular sea, the sea elevation can be assumed statistically stable. See [26] for details and differences between long- and short-crested seas.

in extreme weather conditions. Hence, $R(\psi_L) \approx R(\psi_L + \psi_W)$. From Assumption 1 it follows that $R(\psi_L) \approx R(\psi_y)$, where $\psi_y \cong \psi_L + \psi_W$ denotes the measured heading.

Assumption 3. The time-derivative of the total heading $\dot{\psi}_{tot}$ is small and close to zero (low speed assumption).

We will also exploit the model property that the bias time constant in the x and y directions are equal, i.e., $T_x = T_y$.

At this point, to represent the dynamics of the vessel in a linear form, it is convenient to introduce a new system of vessel parallel coordinates as described in [6, 7, 26]. Vessel parallel coordinates are defined in a reference frame fixed to the vessel, with axes parallel to the earth-fixed frame. In what follows, they will be denote by the upper script p; vector $\eta_L^p \in \mathbb{R}^3$ consists of the LF position (x_L^p, y_L^p) and LF heading ψ_L^p of the vessel expressed in body coordinates, defined as

$$\eta_L^p = R^T(\psi_{tot})\eta_L. \tag{17.17}$$

Computing its derivative with respect to time yields

$$
\begin{aligned}
\dot{\eta}_L^p &= \dot{R}^T(\psi_{tot})\eta_L + R^T(\psi_{tot})\dot{\eta}_L \\
&= \dot{R}^T(\psi_{tot})R(\psi_{tot})\eta_L^p + R^T(\psi_{tot})R(\psi_L)v_L.
\end{aligned}
\tag{17.18}
$$

Using a Taylor series to expand $R^T(\psi_{tot})$ about ψ_L and neglecting the higher order terms, it follows that

$$R^T(\psi_{tot})R(\psi_L) \cong I + \psi_W S, \tag{17.19}$$

where

$$
S = \begin{bmatrix} 0 & 1 & 0 \\ -1 & 0 & 0 \\ 0 & 0 & 0 \end{bmatrix}.
$$

Simple algebraic manipulations yield

$$\dot{R}^T(\psi_{tot})R(\psi_{tot}) = \dot{\psi}_{tot}S. \tag{17.20}$$

From (17.18)–(17.20) it can be concluded that

$$\dot{\eta}_L^p \approx \dot{\psi}_{tot}S\eta_L^p + v_L + \psi_W S v_L. \tag{17.21}$$

We now study the time evolution of the slowly varying bias forces, b, expressed in the vessel parallel coordinates as

$$b^p = R^T(\psi_{tot})b. \tag{17.22}$$

Clearly,

$$b = R(\psi_{tot})b^p, \tag{17.23}$$

and differentiating both sides yields

$$\dot{b} = \dot{R}(\psi_{tot})b^p + R(\psi_{tot})\dot{b}^p. \tag{17.24}$$

From (17.12), (17.23) and (17.24) it follows that

$$\dot{R}(\psi_{tot})b^p + R(\psi_{tot})\dot{b}^p = -T^{-1}R(\psi_{tot})b^p + E_b w_b. \tag{17.25}$$

Reordering (17.25) and multiplying both sides by $R^T(\psi_{tot})$ gives

$$\dot{b}^p = -R^T(\psi_{tot})T^{-1}R(\psi_{tot})b^p - R^T(\psi_{tot})\dot{R}(\psi_{tot})b^p$$
$$+ R^T(\psi_{tot})E_b w_b. \tag{17.26}$$

Using the assumption that $T_x = T_y$, it can be shown that $R^T(\psi_{tot})T = TR^T(\psi_{tot})$; simple algebra also shows that $R^T(\psi_{tot})\dot{R}(\psi_{tot}) = -\dot{\psi}_{tot}S$.

Equation (17.26) can be rewritten as

$$\dot{b}^p = -T^{-1}b^p + \dot{\psi}_{tot}Sb^p + R^T(\psi_{tot})E_b w_b. \tag{17.27}$$

Summarizing the equations above yields

$$\dot{\xi}_\omega = A_\omega(\omega_0)\xi_\omega + E_\omega w_\omega, \tag{17.28}$$

$$\eta_\omega = R(\psi_L)C_\omega\xi_\omega, \tag{17.29}$$

$$\dot{b}^p = -T^{-1}b^p + \dot{\psi}_{tot}Sb^p + R^T(\psi_{tot})E_b w_b, \tag{17.30}$$

$$\dot{\eta}_L^p = \dot{\psi}_{tot}S\eta_L^p + v_L + \psi_W Sv_L, \tag{17.31}$$

$$M\dot{v}_L + Dv_L = \tau + b^p. \tag{17.32}$$

Moreover, using Assumptions 1, 2 and 3 a ***linear model*** is obtained that is given by

$$\dot{\xi}_\omega = A_\omega(\omega_0)\xi_\omega + E_\omega w_\omega, \tag{17.33}$$

$$\eta_\omega^b = C_\omega\xi_\omega, \tag{17.34}$$

$$\dot{b}^p = -T^{-1}b^p + w_b^f, \tag{17.35}$$

$$\dot{\eta}_L^p = v_L, \tag{17.36}$$

$$M\dot{v}_L + Dv_L = \tau + b^p, \tag{17.37}$$

$$\eta_y^f = \eta_L^p + \eta_\omega^b, \tag{17.38}$$

where η_ω^b are WF components of motion in body-coordinate axis, and w_b^f and η_y^f consists of a new modified disturbance and a modified measurement defined by $w_b^f = R^T(\psi_y)E_bw_b$ and $\eta_y^f = R^T(\psi_y)\eta_y$, respectively.[4]

17.2.2   A Brief Review of Three DP Controllers

In what follows we give a short description of three types of controllers used in the current chapter. The first type of controller consists of a nonlinear multivariable PID coupled with a nonlinear passive observer. Passive observers were introduced in the late 1990s; the main motivation for their development was the need to overcome the difficulty of tuning a relatively large number of parameters (through experimental testing of the vessel) in other commonly used approaches such as back-stepping and Kalman filtering, see [5, 30, 31]. In fact, the tuning procedure is simplified significantly using passivity arguments [31]. Moreover, in the absence of measurement noise passive observers satisfy satisfy the property of global convergence, that is, all estimation errors converge to zero. Another interesting property of passive observers is that the wave filtering parameters (filter gains) are functions of the dominating wave frequency, thus making them appropriate candidates for adaptive wave filtering when the sea state and dominating wave frequency are unknown.

In this type of controller, the observer provides estimates of the LF components of the position and the velocity of the vessel which are used in the nonlinear multivariable controller structure. To cover the different sea conditions from calm to extreme seas, we have designed four different controllers and observers based on different values of the dominant wave frequency. For further details on controller design the reader is referred to [21, 26].

The second class of controllers is of the LQG type. It consists of a steady state Kalman filter and a linear quadratic (state-feedback) controller. In order to design the LQG controller, we used the linear model of the vessel presented in (17.33)–(17.38). As in the previous case, four different LQG controllers were designed,

---

[4]When designing observers for wave filtering in dynamic positioning, since the controller regulates the heading of the vessel, the designer can assign a new intensity to w_b^f; however, assigning the intensity of the noise in practice requires considerable expertise.

based on four different dominant wave frequency values, covering different sea conditions from calm to extreme. Details on the design of the LQG DP controllers can be found in [17].

The third type of controller is a robust DP controller designed using $\mathcal{H}_\infty$ and mixed-μ control techniques. In this set-up, the practical assumptions are exploited in order to obtain a linear design model with parametric uncertainties describing the dynamics of the vessel. Appropriate frequency weighting functions are selected to capture the required performance specifications at the controller design phase. The proposed model and weighting functions are then used to design robust controllers. The problem of wave filtering is also addressed during the process of modeling and controller design. As in the previous cases, four $\mathcal{H}_\infty$ robust controllers were designed for different sea conditions. For details on the development of the vessel's model with parametric uncertainty, as well as the procedure adopted for robust DP controller design, the reader is referred to [15, 16].

17.3 Wave Filtering and Control: Numerical Solutions

In what follows we summarize the results of Monte Carlo simulations of wave filtering and dynamic positioning systems. The simulations were carried out using the MCSim. After a short description of the simulator, we evaluate the improvements obtained with the changes in our proposed modified design model. This being done, the DP controllers introduced in Sect. 17.2.2 are evaluated using the simulator.

17.3.1 Overview of the Simulator

The MCSim is a modular, multi-disciplinary simulator based on Matlab/Simulink developed at the Centre for Ships and Ocean Structures, Dept. of Marine Technology, Norwegian Univ. of Science and Technology. The MCSim incorporates high fidelity models, denoted as process plant models or simulation models in [26], at all levels (plants and actuators). It is composed of different modules that include the following:

1. **Environmental module**, containing different wave models, surface current models, and wind models.
2. **Vessel dynamics module**, consisting of a LF and a WF model. The LF model is based on the standard six degrees-of-freedom vessel dynamics, whose inputs are the environmental loads and the interaction forces from thrusters and the external connected systems.
3. **Thruster and shaft module**, containing thrust allocation routine for non-rotating thrusters, thruster dynamics, and local thruster control. It may also include advanced thrust loss models for extreme seas, in which case detailed information about waves, current and vessel motion is required.

4. **Vessel control module**, consisting of different controllers, including nonlinear multivariable PID controllers, for DP.

Details on the MCSim can be found in [8, 22, 23, 29].

In what follows, the results of Monte-Carlo simulations performed with the MCSim are shown to illustrate and assess the performance of a number of different types of observers and controllers for an offshore vessel with DP system. To this effect, in the next section two types of observers based on the two distinct models described by (17.1)–(17.7) and (17.10)–(17.15) are introduced. Their performance is evaluated comparatively under different environmental conditions, from calm to high seas. In the simulations, the environmental conditions are simulated using the JONSWAP spectrum [18]. The study shows the usefulness of the new linear design model adopted. This is followed by a section where the performance obtained with the three types of controllers defined before is also assessed in simulation.

17.3.2 A Comparison of the Modified and Classical Design Models

In this section, in order to compare the usefulness of the two design models described by (17.1)–(17.7) and (17.10)–(17.15), we start by designing a Luenberger-like observer for the model presented by (17.1)–(17.7). After tuning the observer gains (for the best estimation performance), we use the same gains and design another Luenberger-like observer based on the model described by (17.10)–(17.15). The two observers share the same structure (except for the proposed modification) and have the same gains.[5] We compare the estimation results of the two above mentioned observers and reason that better performance with one of the observers reflects the superiority of the model adopted for its design.

To design the observer and optimize the gains we follow the procedure of designing nonlinear passive observer for marine vessels. Passive observers were introduced in [9, 30, 31]. The structure of passive observers for a DP vessel model described by (17.1)–(17.7) is given by

$$\dot{\hat{\xi}}_\omega = A_\omega(\omega_0)\hat{\xi}_\omega + K_1\tilde{\eta}_y, \tag{17.39}$$

$$\hat{\eta}_\omega = C_\omega\hat{\xi}_\omega, \tag{17.40}$$

$$\dot{\hat{b}} = -T^{-1}\hat{b} + K_2\tilde{\eta}_y, \tag{17.41}$$

---

[5]All the gains are optimally tuned for the observer designed using the model described in (17.1)–(17.7). Such a selection favors the old DP model; however, a comparison of the results of simulations shows that the observer designed using the newly proposed model yields better performance.

$$\dot{\hat{\eta}}_L = R(\psi_y)\hat{v}_L + K_3\tilde{\eta}_y, \tag{17.42}$$

$$M\dot{\hat{v}}_L + D\hat{v}_L = \tau + R^T(\psi_y)\hat{b} + R^T(\psi_y)K_4\tilde{\eta}_y, \tag{17.43}$$

$$\hat{\eta}_y = \hat{\eta}_L + \hat{\eta}_\omega. \tag{17.44}$$

For details on nonlinear passive observers and the selection of the observer gains, i.e., K_i, $i = 1\ldots 4$, the reader is referred to [5, 6, 9, 19, 26, 30–32].

The structure of the second observer for a DP vessel model described by (17.10)–(17.15) (i.e., observer based on the new proposed DP model) is adopted from the one in (17.39)–(17.44) except for the WF motion that is now expressed in body coordinates as

$$\hat{\eta}_\omega = R(\psi_y)C_\omega\hat{\xi}_\omega. \tag{17.45}$$

In conclusion, throughout this section we use the same set of gains in order to ascertain the impact of the design model on the performance obtained with the observers. Three different environment conditions from calm to high seas are considered, and for each one a separate observer is designed. Table 17.1 shows the definition of the sea condition associated with a particular model of supply vessel that is used in the MCSim.

For simulation purposes, the nominal values for the dominant wave frequency are selected as $\{0.48, 0.63, 0.92\}$ (rad/s). Figures 17.2 and 17.3 show the time evolution of total motion and the LF component of the motion and their estimates by two passive observers [one based on the model (17.1)–(17.7) and the other based on the modified model (17.10)–(17.15)] in a high sea state condition. The simulation is done in a station keeping scenario where a nonlinear multivariable PID controller regulates the position and heading of the vessel about zero. It is seen that even with wave filtering, some of the 1st-order wave frequency components are present in the LF estimates.[6] However, the simulations support the conclusion that the observer proposed in this chapter yields very good performance when compared with that obtained with the passive observer described in [9]. To quantify the potential performance improvement of our modified observer over the passive observer of [9], we introduce "percentage comparison" figure of merit given by

$$\%E = \frac{|\mathrm{VAR}_{\tilde{p}_L^{old}}| - |\mathrm{VAR}_{\tilde{p}_L^{new}}|}{|\mathrm{VAR}_{\tilde{p}_L^{new}}|} \times 100, \tag{17.46}$$

---

[6]At this point, we should emphasize that the observers are designed according to the simple model of (17.10)–(17.15) [and (17.1)–(17.7)] while they are tested in the MCSim using a high fidelity model which captures hydrodynamic effects, generalized coriolis and centripetal accelerations, nonlinear damping and current forces, and generalized restoring forces. Moreover, in the MCSim the JONSWAP wave spectrum is used to simulate the waves while the observers are designed using a linear second order approximation of the spectrum.

Table 17.1 Definition of sea states from [24]

| Sea state	Dominant wave frequency ω_0 (rad/s)	Significant wave height H_s (m)
Calm seas	>1.11	<0.1
Moderate seas	[0.74 1.11]	[0.1 1.69]
High seas	[0.53 0.74]	[1.69 6.0]
Extreme seas	<0.53	>6.0
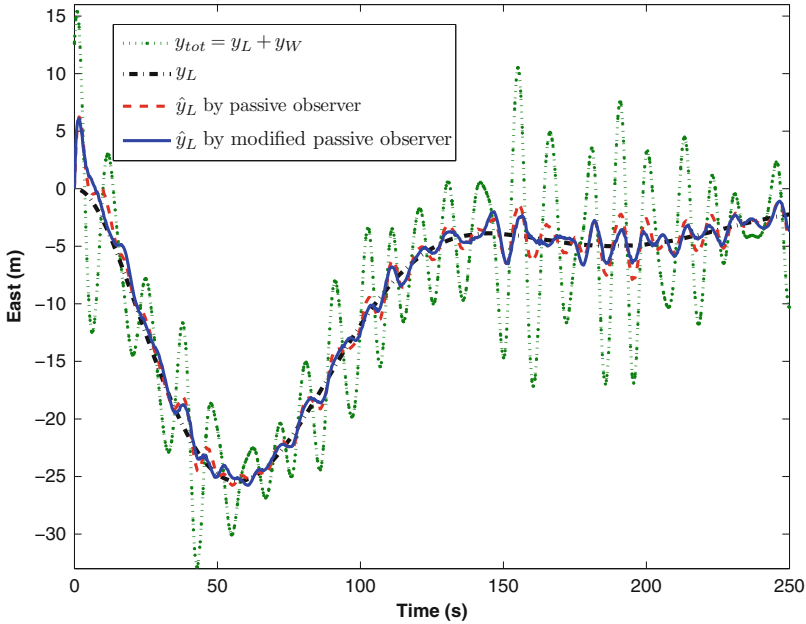
Fig. 17.2 Total motion, LF component of a (typical 100 m long) DP vessel (only sway), and its estimates

where $\text{VAR}_{\tilde{p}}$ is the variance of $\tilde{p}$, $\tilde{p}_L^{old}$ and $\tilde{p}_L^{new}$ are the estimation error of p_L with the passive observer of [9] and our modified observer, respectively, and finally p_L is the LF component of the motion in surge, sway or yaw.

Table 17.2 summarizes the result of Monte-Carlo simulations with different environment conditions from calm to high seas where a nonlinear multivariable PID controller regulates the position of the ship at origin. We have computed the performance improvement of our modified observer over that described in [9].

Table 17.3 shows similar results when the vessel position was commanded to change 300 m forward in surge and sway while keeping the heading at zero; this simple maneuver was executed with the nonlinear multivariable PID control law referred to above. As Tables 17.2 and 17.3 show, as the sea condition changes from calm to high seas, there is significant performance improvement with the use of the new proposed observer, when compared with that of the passive observer in [9].
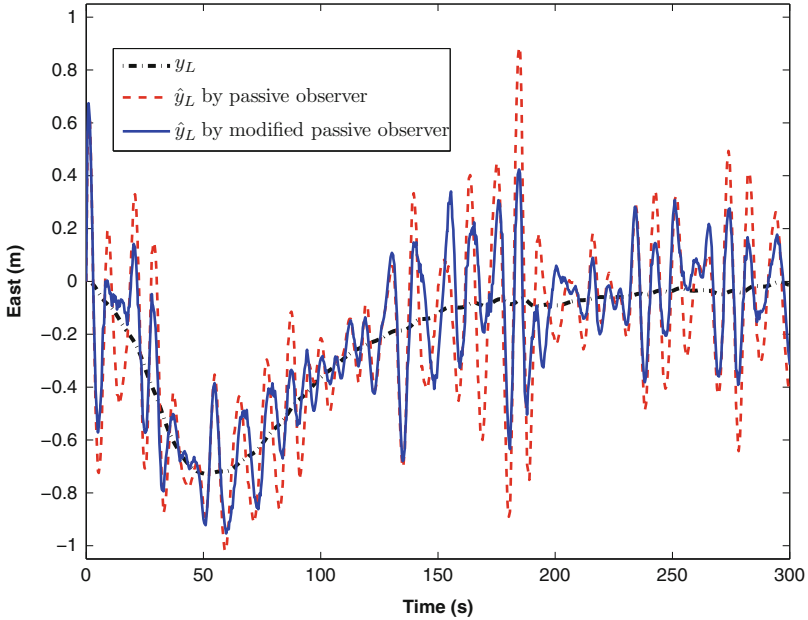
Fig. 17.3 LF component of a (typical 100 m long) DP vessel (only sway), and its estimates

Table 17.2 Performance improvements of new observer (station keeping)

	Calm seas	Moderate seas	High seas
%E in surge	16 %	18 %	78 %
%E in sway	22 %	25 %	115 %
%E in yaw	−9 %	51 %	93 %

Table 17.3 Performance improvements of new observer (Manoeuvering)

	Calm seas	Moderate seas	High seas
%E in surge	17 %	18.5 %	80 %
%E in sway	24 %	27 %	115 %
%E in yaw	−8 %	51 %	94 %

The reason for this behavior is the violation of Assumption 2 with the observer in [9]. In fact, when shifting from calm sea to moderate and high sea conditions, the amplitude of the wave-induced yaw motion becomes larger and neglecting this term causes performance degradation. This problem is alleviated in our proposed observer (by modeling the WF motion in the body frame).

Now that the efficacy of the newly proposed design model has been shown we will continue, in what follows, by presenting the result of numerical simulations with three different types of DP controllers designed based on the new model.

17.3.3 Numerical Simulations with Three Types of DP Controllers

This section summarizes the results of Monte-Carlo simulations aimed at assessing the performance achievable with the three types of controllers described before. In parallel, we study the performance of the wave filters designed using the newly proposed model, when used in conjunction with the first and second controllers of Sect. 17.2.2. In the simulations, the different environment conditions from calm to extreme seas were simulated using the JONSWAP spectrum [18]. Notice that in addition to the three environment conditions (calm, moderate, and high sea) used in Sect. 17.3.2 we also consider the extreme sea state, see Table 17.1.

We start by comparing the estimation-performance of the wave filters when run together with the first two controllers.[7] At this point in the simulation, the nominal values for the dominant wave frequency were selected as $\{0.48, 0.63, 0.92, 1.18\}$ (rad/s). Figure 17.4 shows the vessel's total and low frequency motion components using a passive-like observer (that is run with a nonlinear PID controller) and a Kalman filter (inserted in an LQG observer/controller structure) in a calm sea state. The simulation is done in a station keeping scenario where a nonlinear multivariable PID controller (in conjunction with a passive observer) and a LQG controller (which includes a Kalman filter in its structure) regulate the position and heading of the vessel about zero. To allow for a better estimation-performance comparison, in Fig. 17.5 we only show the LF component of the motion and its estimates by the passive observer and a Kalman filter in calm sea state (for the same simulation as the one shown in Fig. 17.4). It is seen that the Kalman filter is better (in terms of estimating the LF components of motion) than the passive observer. Figures 17.6 and 17.7 show the results of similar simulations for moderate and high seas. The results support the observation that the Kalman filter has better wave filtering properties (estimation of the LF part of the motion) when compared to the passive observer. Moreover, it is also seen that even with wave filtering, some of the 1st-order wave frequency components are seen in the LF estimates. Figures 17.8, 17.9, and 17.10 focus on the motion control capabilities, and illustrate the performance obtained with the DP controllers mentioned before, under different sea conditions.[8] Here we should highlight that in Figs. 17.8, 17.9, 17.10, and 17.11 we present only the LF components of motion. These simulations suggest that the LQG has the best performance in terms of regulating the LF components of motion and the robust controller has the worst performance overall. Notice that the robust controller does not include any observer to estimate the LF motions and the controllers are fed with the total position (LF+WF). However, if the comparison is done in terms of total vessel motion (LF+WF), the robust controller exhibits superior dynamic

---

[7]Wave filtering in the robust DP controller is not implemented explicitly, see [15, 16] for details.

[8]All the results are presented in full scale. During the testing phase care was taken to ensure that all controllers were tuned to their best performance, so as to allow for a fair comparative study.
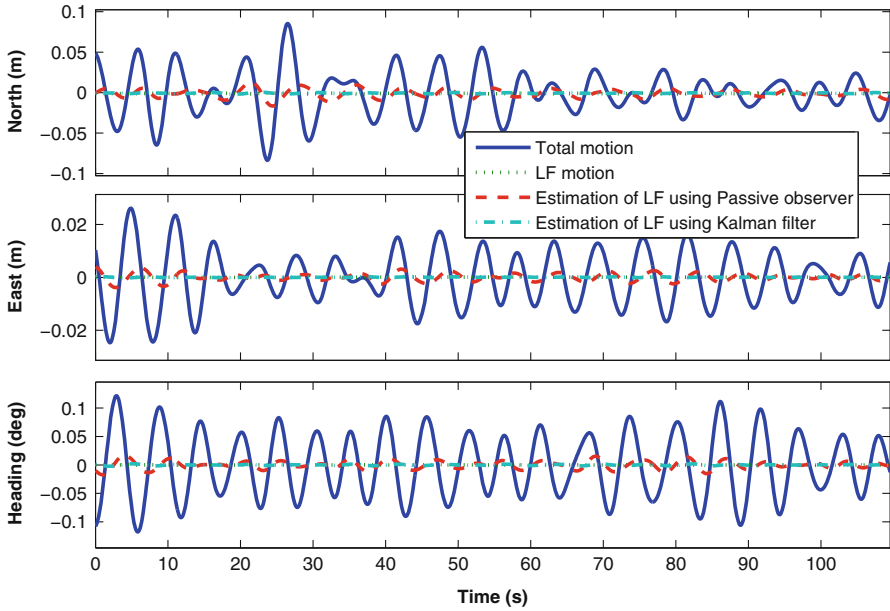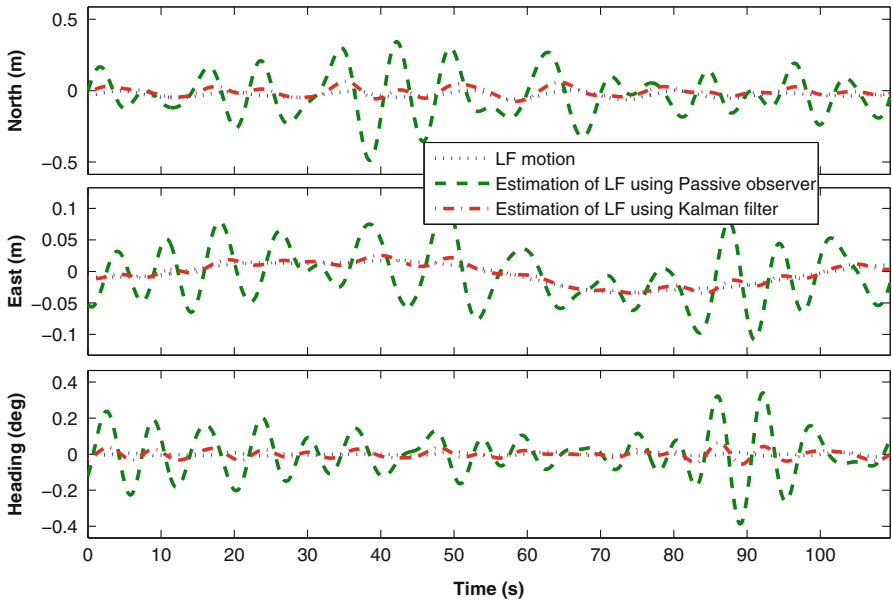
Fig. 17.4 Numerical simulations (calm sea): total motion of the vessel, LF components of motion, and estimation of the LF motion with a passive observer and a Kalman filter
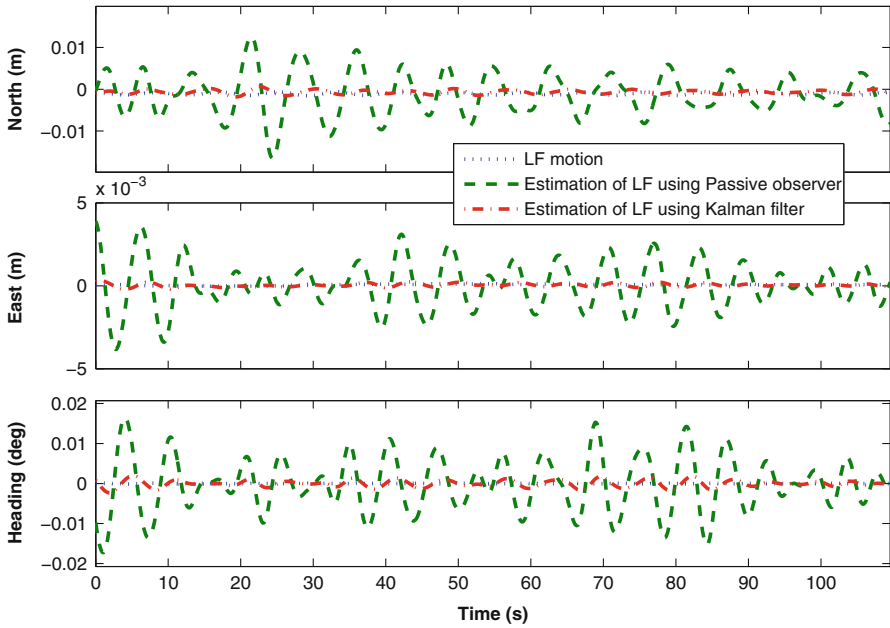
Fig. 17.5 Numerical simulations (calm sea): LF components of motion and estimation of the LF motion with a passive observer and a Kalman filter (a zoom in on Fig. 17.4)
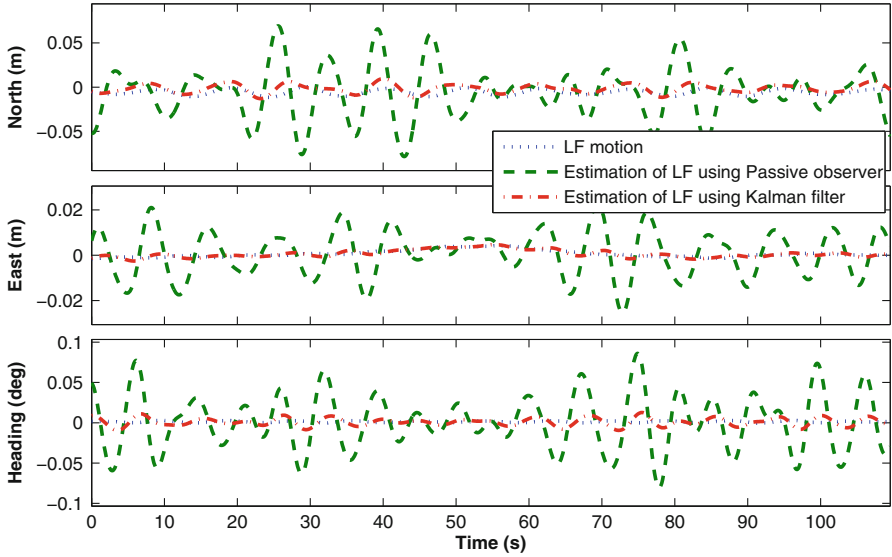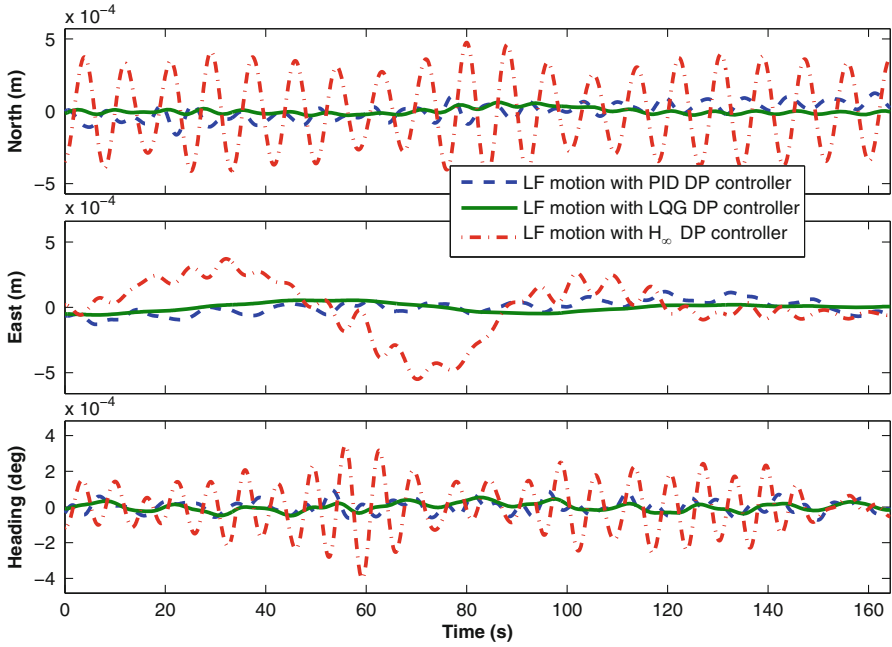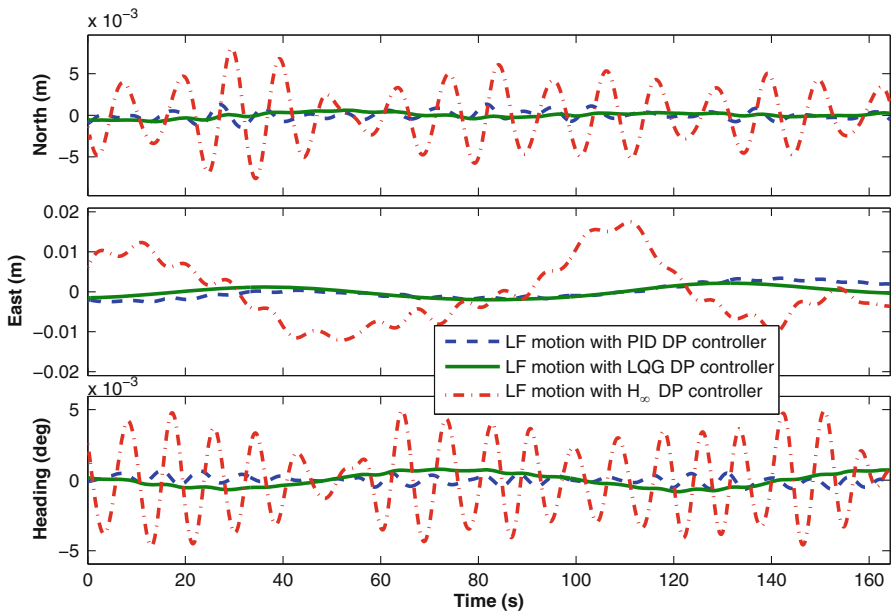
Fig. 17.6 Numerical simulations (moderate sea): LF components of motion and estimation of the LF motion with a passive observer and a Kalman filter

Fig. 17.7 Numerical simulations (high sea): LF components of motion and estimation of the LF motion with a passive observer and a Kalman filter

Fig. 17.8 Numerical simulations (calm sea): LF components of motion of the vessel operating with different DP controllers
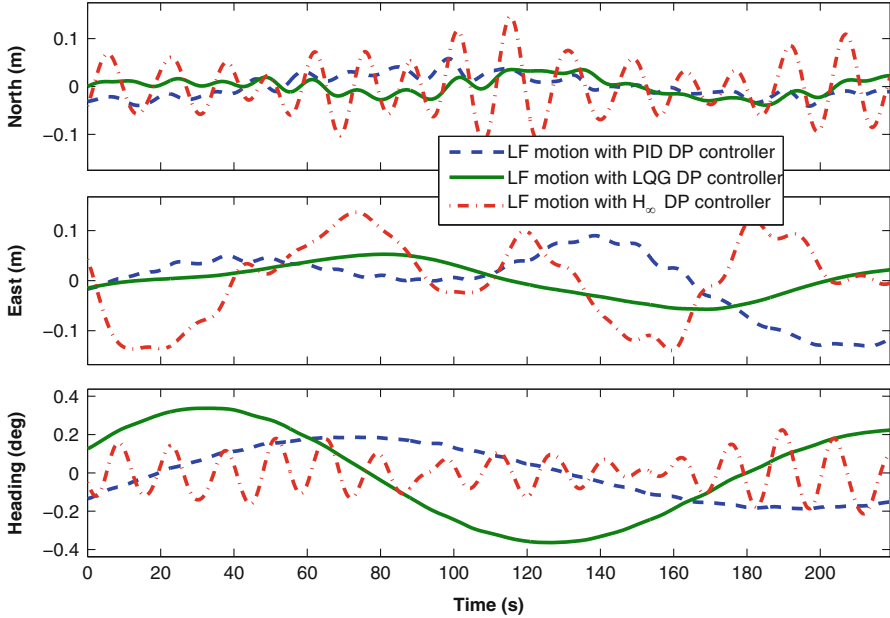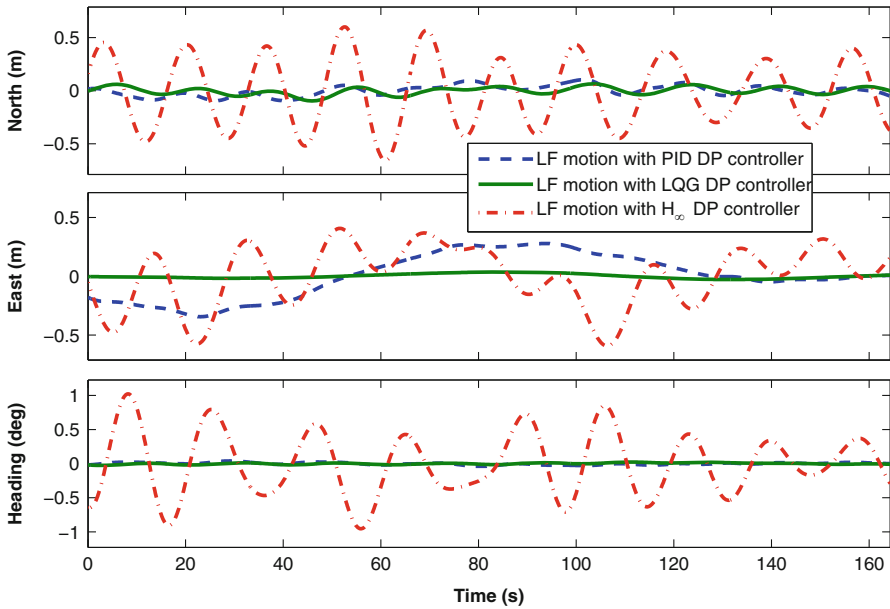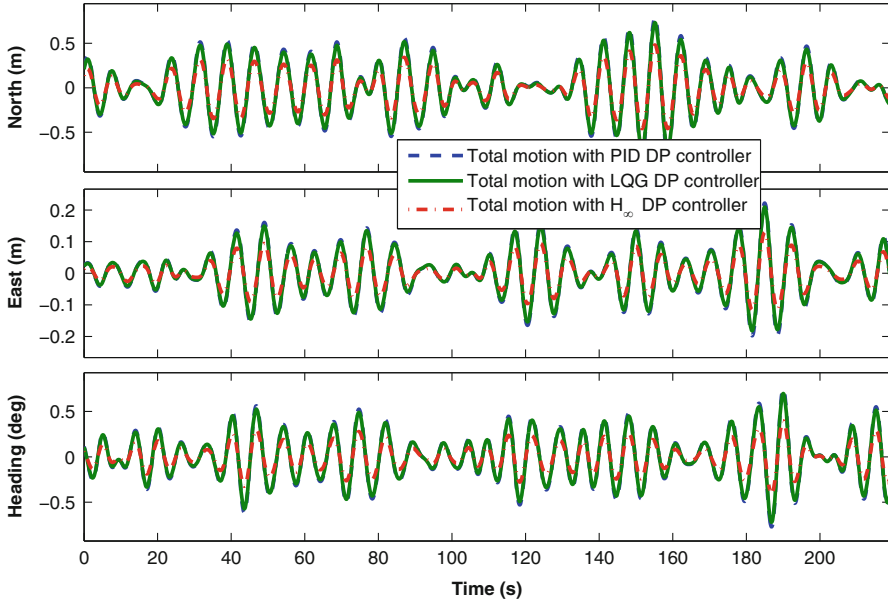

Fig. 17.9 Numerical simulations (moderate sea): LF components of motion of the vessel operating with different DP controllers

Fig. 17.10 Numerical simulations (high sea): LF components of motion of the vessel operating with different DP controllers

Fig. 17.11 Numerical simulations (extreme sea): LF components of motion of the vessel operating with different DP controllers
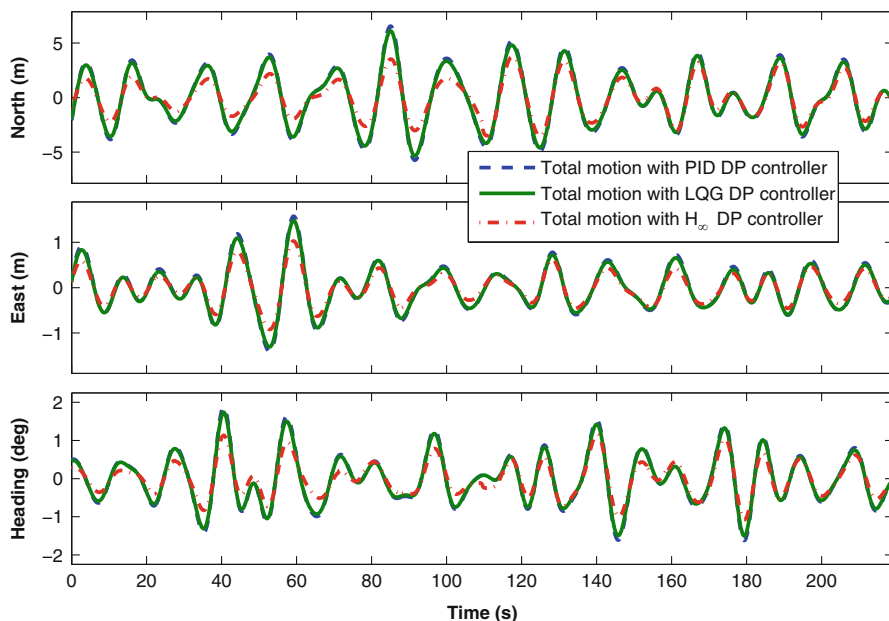
Fig. 17.12 Numerical simulations (moderate sea): total motion of the vessel with different DP controllers

positioning with respect to that obtained with the other two types of controllers (that show similar performance), see Figs. 17.12 and 17.13. This is due to the poor wave filtering of the robust controllers and the fact that the robust controllers (without an explicit wave filter) try to regulate all the motions of the vessel (and not only the LF part). Notice that in extreme seas or swell with very long wave periods, wave filtering is turned off as described in [17, 21, 27] and the DP controllers should regulate the total motion of the vessel (and not only the LF part), and hence, robust controllers will be favorable in extremes seas.

17.4 Experimental Model Testing Results

This section bridges the gap between theory and practice. To this effect, we assess the performance of the three types of controllers described before using an experimental set-up consisting of the Cybership III model vessel of the Marine

Fig. 17.13 Numerical simulations (extreme sea): total motion of the vessel with different DP controllers

Cybernetics Laboratory (MCLab), Department of Marine Technology, Norwegian University of Science and Technology (NTNU). During the tests, different sea conditions were emulated using a hydraulic wave maker.

17.4.1 Overview of the Cybership III

Cybership III is a 1:30 scaled model of an offshore vessel operating in the North Sea. Table 17.4 presents the main parameters of both the model and the full scale vessel.

Cybership III is equipped with two pods located at the aft. A tunnel thruster and an azimuth thruster are installed at the bow.[9] The vessel has mass m = 75 kg, length L = 2.27 m and breadth B = 0.4 m. The main parameters of the model are presented in Table 17.4. The internal hardware architecture is controlled by an onboard computer that communicates with the onshore PC through a WLAN. The PC onboard the ship uses QNX real-time operating system (target PC). The control system is developed on a PC in the control room (host PC) under Simulink/Opal and downloaded to the target PC using automatic C-code generation and wireless

---

[9]For technical reasons in this experiment the tunnel thruster was deactivated.

Table 17.4 Model main parameters

|	Model	Full scale
Overall length	2.275 m	68.28 m
Length between perpendiculars	1.971 m	59.13 m
Breadth	0.437 m	13.11 m
Breadth at water line	0.437 m	13.11 m
Draught	0.153 m	4.59 m
Draught front perpendicular	0.153 m	4.59 m
Draught aft. perpendicular	0.153 m	4.59 m
Depth to main deck	0.203 m	6.10 m
Weight (hull)	17.5 kg	Unknown
Weight (normal load)	74.2 kg	22.62 tons
Longitudinal center of gravity	100 cm	30 m
Vertical center of gravity	19.56 cm	5.87 m
Propulsion motors max shaft power (6 % gear loss)	81 W	3200 HP
Tunnel thruster max shaft power (6 % gear loss)	27 W	550 HP
Maximum speed	Unknown	11 knots

Ethernet. The motion capture unit, installed in the MCLab, provides Earth-fixed position and heading of the vessel. The motion capture unit consists of onshore 3-cameras mounted on the towing carriage and a marker mounted on the vessel. The cameras emit infrared light and receive the light reflected from the marker.

To emulate the sea conditions, a hydraulic wave maker system is used. It consists of a single flap covering the whole breadth of the basin, and a computer controlled motor, moving the flap. The device can produce regular and irregular waves with different spectrums. We have used the JONSWAP spectrum to simulate the different sea conditions for our experiments, see [18].

17.4.2 Model Testing Results

Figure 17.14 shows the vessel position and heading in a moderate sea condition. The results of the model test are in agreement with the ones obtain in the numerical simulation study, showing satisfactory performance of wave filtering (estimating the LF part of the motion) for both the passive observer and the Kalman filter. However, the Kalman filter yields a smoother estimate of the LF vessel motion, as shown in Fig. 17.15 that is a zoom-in on Fig. 17.14 (we omit the total motion in Fig. 17.15 for the sake of a better comparison). It is seen that the Kalman filter provides smoother estimation of the LF part of motion.
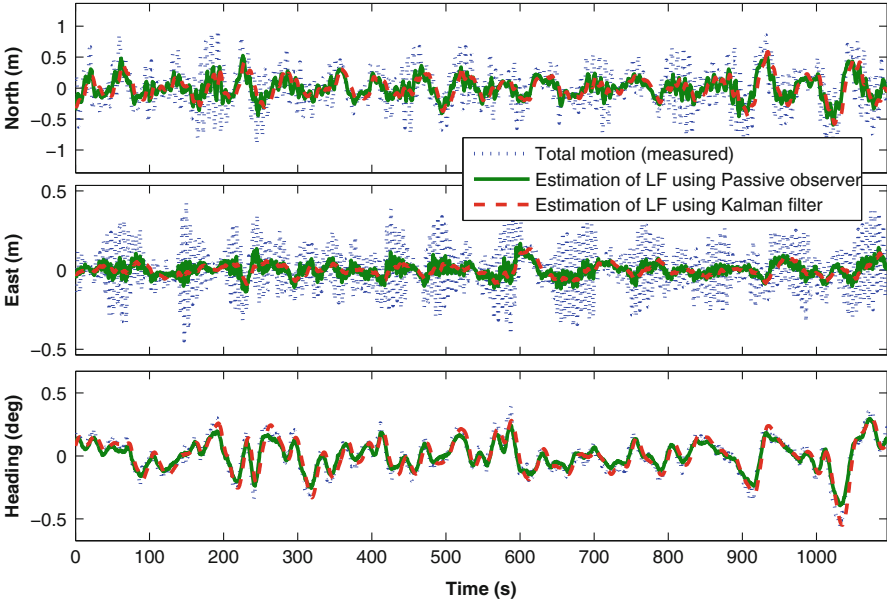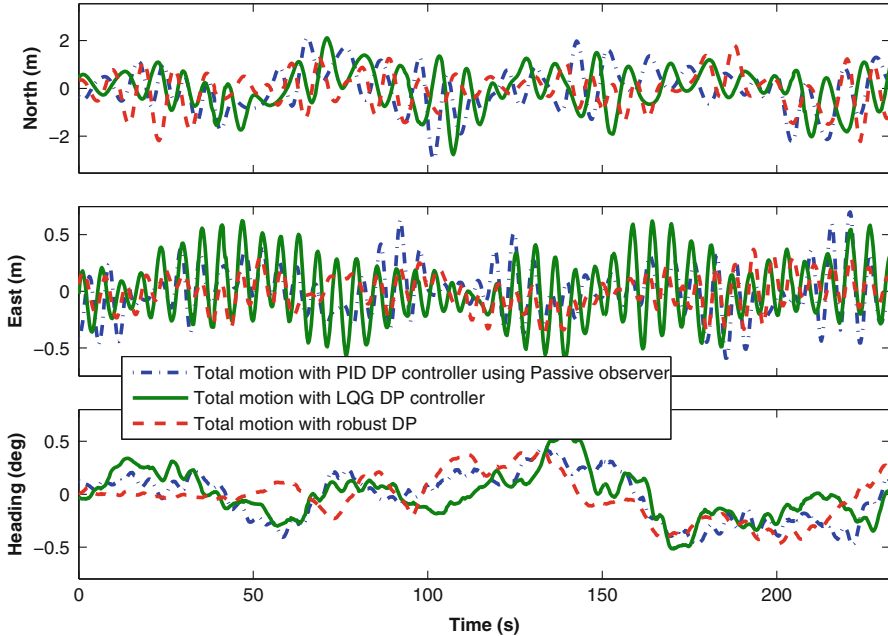
Fig. 17.14 Experimental results (moderate sea): total motion of the vessel and estimation of the LF components of motion with a passive observer and a Kalman filter
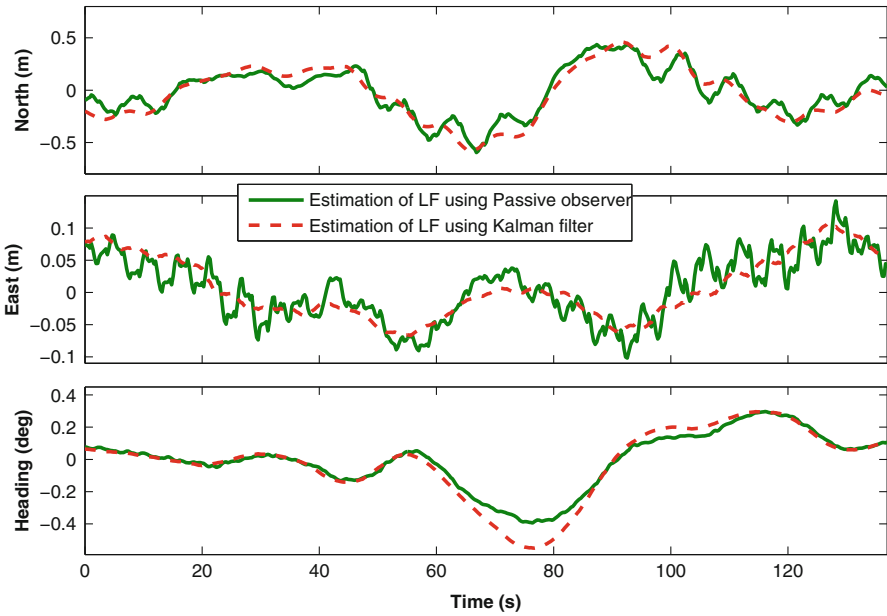
Fig. 17.15 Experimental results (moderate sea): estimation of the LF components of motion with a passive observer and a Kalman filter (zoom in of Fig. 17.14)

Fig. 17.16 Experimental results (high sea): total motion of the vessel with different DP controllers

Table 17.5 Experimental results (high sea): calculated covariance of total motion of the vessel (average of three experiments)

	x (m)	y (m)	ψ (deg)
PID with a passive observer	0.80	0.03	0.05
LQG controller	0.74	0.07	0.04
robust controller	0.62	0.02	0.09

Figure 17.16 shows the comparison of the total motion of the vessel in high sea, working under different DP systems; notice that the robust DP controller has a (slightly) better performance in the regulation of the vessel and the two other controllers have similar performance. Table 17.5 shows the mean covariance of three station keeping experiments with the above mentioned controllers. The table also shows that the robust DP controller has better performance (in terms of x_{tot} and y_{tot} regulation, but not in ψ_{tot}) in the station keeping scenario, when compared with the other two controllers.

17.5 Combined Framework in Transport of Water and Transport over Water

This chapter is focused on the development of a new linear model of marine vessels subjected to currents and sea waves. This is a key step in devising solutions to the problem of dynamic positioning and wave filtering of vessels for scientific and

commercial operations. The model proposed captures the influence of forces and moments due to currents and sea waves. The effect of sea waves includes two terms: (a) oscillatory forces and moments and (b) slowly varying forces and moments (modeled together with the forces and moment due to currents). Notwithstanding the simplicity of the model, it captures the physics of the problem at hand in an effective manner. Hence, it is at the heart of the application of new techniques in control and estimation theory to the design of wave filters and controllers for DP systems. Most marine vessels equipped with DP systems operate in open seas where flow control is impossible. However, some passenger, cruise, and commercial vessels with DP systems also travel in open channels where transport of water and flow control are clearly feasible. Should the need arise for the use of DP systems in such circumstances, the information received from the control system that regulates transport of water in open canal networks can in principle be used to update the proposed model to use higher fidelity models of currents to best capture the effect of the latter on the vessel. This combined framework of transport of and over water could potentially improve the performance of DP systems and speed up their initialization process.[10]

17.6   Conclusions and Future Research

This chapter proposed a new linear design model for marine vessels subjected to ocean waves and currents, with application to wave filtering and dynamic positioning. Its key contribution was the development of a modified linear model that captures the physics of the vessel in a simple, yet effective manner. Numerical simulations, carried out using a high fidelity nonlinear dynamic positioning (DP) simulator, showed the performance improvement in wave filtering due to the use of the modified model in comparison with commonly used models. The proposed model is instrumental in applying new techniques in control and estimation theories to the problem of DP as shown in [14–17] for simulation and model testing. The chapter offered also a comprehensive evaluation of the performance obtained with a set of three DP controllers designed for different sea conditions, for a representative vessel model. The evaluation included Monte-Carlo simulations, as well as model-test experiments with a vessel in a towing tank equipped with a wave making system. The results obtained confirmed that Kalman filter exhibits superior performance in wave filtering. Moreover, they also showed that robust DP controller has better performance in the regulation of the total motion of the vessel (LF+WF). However, a PID controller equipped with a passive observer was the simplest controller to design and tune. Future work will include the application of the methodologies developed to the design of DP controllers for a real vessel.

---

[10]Before a DP system is functional, the state estimate of the filter in the DP system should converge to its steady state performance; this initialization may take tens of minutes.

References

1. Balchen J, Jenssen NA, Sælid S. Dynamic positioning using Kalman filtering and optimal control theory. In: The IFAC/IFIP symposium on automation in offshore oil field operation, Bergen, 1976. p. 183–6.
2. Balchen J, Jenssen NA, Sælid S. Dynamic positioning of floating vessels based on Kalman filtering and optimal control. In: Proceedings of the 19th IEEE conference on decision and control, New York, 1980. p. 852–64.
3. Balchen J, Jenssen NA, Sælid S. A dynamic positioning system based on Kalman filtering and optimal control. Modeling, Identification and Control (MIC). 1980;1(3):135–63.
4. Faltinsen OM. Sea loads on ships and offshore structures. Cambridge: Cambridge University Press; 1990.
5. Fossen TI. Nonlinear passive control and observer design for ships. Modeling, Identification and Control (MIC). 2000;21(3):129–84.
6. Fossen TI. Handbook of marine craft hydrodynamics and motion control. Chichester: Wiley; 2011.
7. Fossen TI, Perez T. Kalman filtering for positioning and heading control of ships and offshore rigs. IEEE Control Syst Mag. 2009;29(6):32–46.
8. Fossen TI, Perez T. Marine systems simulator (MSS). 2009. http://www.marinecontrol.org/.
9. Fossen TI, Strand JP. Passive nonlinear observer design for ships using lyapunov methods: Full-scale experiments with a supply vessel. Automatica. 1999;35:3–16.
10. Fossen TI, Sagatun SI, Sørensen AJ. Identification of dynamically positioned ships. J Control Eng Pract. 1996;4(3):369–76.
11. Grimble MJ, Patton RJ, Wise DA. The design of dynamic ship positioning control systems using stochastic optimal control theory. Optim Control Appl Methods. 1980;1:167–202.
12. Grimble MJ, Patton RJ, Wise DA. The design of dynamic ship positioning control systems using stochastic optimal control theory. IEE Proc. 1980;127(3):93–102.
13. Grøvlen Å, Fossen TI. Nonlinear control of dynamic positioned ships using only position feedback: An observer backstepping approach. In: Proceedings of the IEEE conference on decision and control (CDC'96), Kobe, 1996.
14. Hassani V, Sørensen AJ, Pascoal AM. Evaluation of three dynamic ship positioning controllers: from calm to extreme conditions. In: Proceedings of the NGCUV'12 - IFAC workshop on navigation, guidance and control of underwater vehicles, Porto, 2012.
15. Hassani V, Sørensen AJ, Pascoal AM. Robust dynamic positioning of offshore vessels using mixed-μ synthesis. Part I: Designing process. In: Proceedings of ACOOG'12 - IFAC workshop on automatic control in offshore oil and gas production, Trondheim, 2012.
16. Hassani V, Sørensen AJ, Pascoal AM. Robust dynamic positioning of offshore vessels using mixed-μ synthesis. Part II: Simulation and experimental results. In: Proceedings of ACOOG'12 - IFAC workshop on automatic control in offshore oil and gas production, Trondheim, 2012.

17. Hassani V, Sørensen AJ, Pascoal AM, Pedro Aguiar A. Multiple model adaptive wave filtering for dynamic positioning of marine vessels. In: Proceedings of ACC'12 - American control conference, Montreal, 2012.

18. Hasselmann K, Barnett TP, Bouws E, Carlson H, Cartwright DE, Enke K, Ewing JA, Gienapp H, Hasselmann DE, Kruseman P, Meerburg A, Müller P, Olbers DJ, Richter K, Sell W, Walden H. Measurements of wind-wave growth and swell decay during the joint north sea wave project (JONSWAP). Ergnzungsheft zur Deutschen Hydrographischen Zeitschrift Reihe. 1973;8(12):1–95.

19. Loria A, Fossen TI, Panteley E. A separation principle for dynamic positioning of ships: theoretical and experimental results. IEEE Trans. on Contr. Syst. and Tech. 2000;8(2): 332–43.

20. MARINTEK. Marine cybernetics laboratory. 2014. http://www.sintef.no/home/MARINTEK/Laboratories/Marine-Cybernetics-Laboratory/. Accessed 31 July 2014 [Online].

21. Nguyen TD, Sørensen AJ, Quek ST. Design of hybrid controller for dynamic positioning from calm to extreme sea conditions. Automatica. 2007;43(5):768–85.

22. Perez T, Smogeli ØN, Fossen TI, Sørensen AJ. An overview of marine systems simulator (MSS): A simulink toolbox for marine control systems. In: Proceedings of Scandinavian conference on simulation and modeling (SIMS'05), Trondheim, 2005.

23. Perez T, Sørensen AJ, Blanke M. Marine vessel models in changing operational conditions – a tutorial. In: 14th IFAC symposium on system identification (SYSID'06), Newcastle, 2006.

24. Price WG, Bishop RED. Probabilistic theory of ship dynamics. London: Chapman and Hall; 1974.

25. Sælid S, Jenssen NA, Balchen J. Design and analysis of a dynamic positioning system based on Kalman filtering and optimal control. IEEE Transactions on Automatic Control. 1983;28(3):331–9.

26. Sørensen AJ. Lecture notes on marine control systems. Technical Report UK-11-76, Norwegian University of Science and Technology, 2011.

27. Sørensen AJ. A survey of dynamic positioning control systems. Annual Reviews in Control. 2011;35:123–36.

28. Sørensen AJ, Sagatun SI, Fossen TI. Design of a dynamic positioning system using model-based control. J Control Eng Pract. 1996;4(3):359–68.

29. Sørensen AJ, Pedersen E, Smogeli Ø. Simulation-based design and testing of dynamically positioned marine vessels. In: Proceedings of international conference on marine simulation and ship maneuverability (MARSIM'03), Kanazawa, 2003.

30. Strand JP. Nonlinear position control systems design for marine vessels. Ph.D. thesis, Dept. of Eng. Cybernetics, Norwegian University of Science and Technology, Trondheim, 1999.

31. Strand JP, Fossen TI. Nonlinear passive observer for ships with adaptive wave filtering. In: Nijmeijer H, Fossen TI, editors. New directions in nonlinear observer design. London: Springer; 1999. p. 113–34.

32. Torsetnes G, Jouffroy J, Fossen TI. Nonlinear dynamic positioning of ships with gain-scheduled wave filtering. In: Proceedings of the IEEE conference on decision and control (CDC'04), Paradise Iceland, 2004.

33. Triantafyllou MS. Cable mechanics for moored floating systems. In: Proceedings of 7th international conference on the behaviour of offshore structures at sea (BOSS'94), Cambridge, 1994. p. 57–77.